Available online at www.sciencedirect.com
ScienceDirect
International Journal of Heat and Mass Transfer 51 (2008) 1049–1060
International Journal of HEAT and MASS TRANSFER
www.elsevier.com/locate/ijhmt

A simplistic model to study the influence of film cooling on low temperature hot corrosion rate in coal gas/syngas fired gas turbines

Vaidyanathan Krishnan, Sanjeev Bharani, J.S. Kapat *, Y.H. Sohn, V.H. Desai

Mechanical, Materials and Aerospace Engineering Department, University of Central Florida, Orlando, FL 32816, United States

Received 13 October 2006; received in revised form 25 May 2007
Available online 30 July 2007

Abstract

The present paper is an attempt to establish an analytical study of low temperature hot corrosion (LTHC) in the context of high temperature turbines using coal gas or syngas with trace amount of sulfur in the fuel. LTHC in the presence of film cooling is explored using a simple analytical approach and heat and mass transfer analogy with film cooling air temperatures from 450 °C to 550 °C, hot gas stream temperature of 1425 °C and 0.5% of sulfur concentration in the fuel. For all the cooling air temperatures studied here, film cooling augments corrosion when the mainstream velocity is high. However, reduction in the mainstream velocity results in the suppression of corrosion after employing film cooling. A sharp peak in corrosion rate close to the cooling hole ($<10s$) is also seen. As the base super alloy is vulnerable to hot corrosion in this region, designers should consider the high corrosion rate seriously. The present model provides a simple baseline prediction methodology and sets direction for optimization needs.

Keywords: Low temperature hot corrosion; Gas turbine; Sulfidation; Modeling

1. Introduction

The concept of coal gas or syngas based Integrated Gasification Combined Cycle (IGCC) gas turbine power plants have drawn considerable interest in recent years. These power plants have shown significant potential for meeting the ever-increasing power demands as well as stricter environmental regulations. The trouble free operational life of such a power plant is limited due to many factors that lead to material failure of the blades. Out of these factors, hot corrosion [1] of metallic alloys is a major concern. The super alloys used for manufacturing of turbine components are susceptible to hot corrosion attack to some extent. There has been significant development in super alloys and thermal barrier coating (TBC) [2] in the recent years for natural gas based heavy frame gas turbines for power generation. However, not much has been achieved for coal gas or syngas based gas turbines such as the ones proposed for IGCC systems.

Analysis of hot corrosion of alloys posses much difficulty, as the degradation mechanisms are quite complex and time dependent. However, examination of hot corrosion data obtained as a function of time shows two distinct stages of attack. These are an initial stage during which the attack is not too severe and a later propagation stage during which the attack is substantially increased. These stages are dependent on the alloy composition, temperature, gas composition, salt/deposit composition and deposition rate. Hitherto, the mechanism of hot corrosion has been investigated in a much simpler way, which is not directly applicable to gas turbines in the presence of film cooling flow. The present paper is a step ahead mainly focused on the effect of temperature and salt deposition rate (particularly for sulfur derived salts) in the presence of film cooling.

* Corresponding author. Tel.: +1 407 823 2179; fax: +1 407 823 0208.
E-mail address: jkapat@mail.ucf.edu (J.S. Kapat).

0017-9310/$ - see front matter © 2007 Elsevier Ltd. All rights reserved.
doi:10.1016/j.ijheatmasstransfer.2007.05.017

Nomenclature

C_p	specific heat at constant pressure
M	blowing ratio
Nu	Nusselt Number
Pr	Prandtl number
Re	Reynolds number
Sc	Schmidt number
Sh	Sherwood number
T	temperature
U	average velocity
h	heat transfer coefficient
h_m	mass transfer coefficient
j	SO_2 mass flux
k	conductivity
q''	heat flux
s	slot width
t	thickness
x	distance downstream from hole

Greek symbols

ϕ	mass fraction
η	film cooling effectiveness
η_c	film protection effectiveness
ρ	density

Subscripts

I	inconel plate
aw	adiabatic wall
c	coolant
d	dew point
f	fluid
iw	impermeable wall
r	recovery
ref	reference value
x	distance downstream from hole
w	wall
∞	free stream
0	no film cooling
1	with film cooling

In hot corrosion, operating temperatures (Fig. 1) govern the mechanism to a large extent. Studies show that the degradation due to hot corrosion is particularly high at two temperatures. At first it appears at approximately 700 °C and is referred to as LTHC or type II hot corrosion, normally found in land and marine based gas turbine power plants. The other high degradation appears at temperatures between 850 °C and 1000 °C. This is called high temperature hot corrosion (HTHC), or type I hot corrosion, which is observed mostly in aircraft engines.

It is important to note that for hot corrosion to occur presence of sulfur based compounds (Fig. 2) are essential. Especially at elevated temperatures a substantial amount of sulfide phases have been reported beneath the deposits obtained on turbine components [1]. The sulfides begin to oxidize and the resulting phases degrade the base alloys, as observed in the hot corrosion of alloys in gas turbines (Fig. 3). Over the years, researchers have tried to understand the influence of various parameters affecting hot corrosion in the absence of film cooling. The complexity of the analysis is further increased due to the presence of film cooling air on the turbine surfaces.

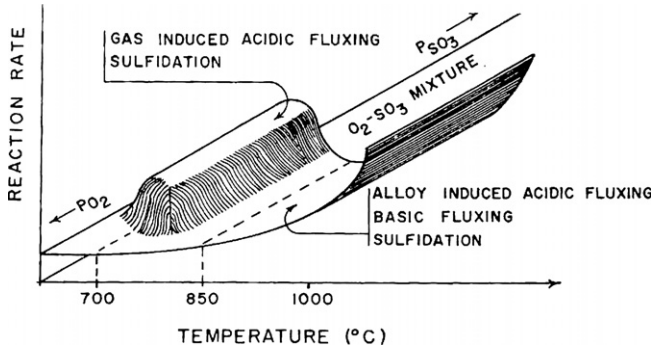

Fig. 1. Hot corrosion: temperature dependence [1].

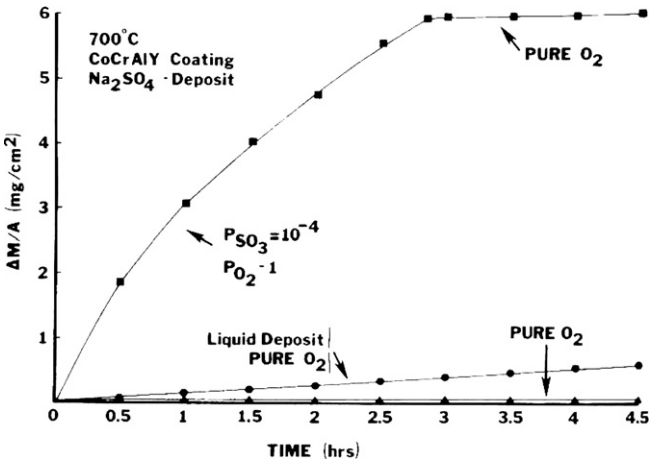

Fig. 2. Hot corrosion-dependence on sulfur (SO_3 obtained from SO_2 and O_2) [1].

Film cooling [3] is a widely used cooling method to keep the temperature of components in the hot gas path within a suitable limit. In depth understanding has been acquired in this technique, which helps in increasing operating life of gas turbines. However, not much has been reported on how hot corrosion is affected in the presence of film cooling. When secondary air flow at a relatively lower temperature is injected over a metal component it not only decreases the temperature of the surface, but also has the tendency to reduce the concentration of sulfur compounds,

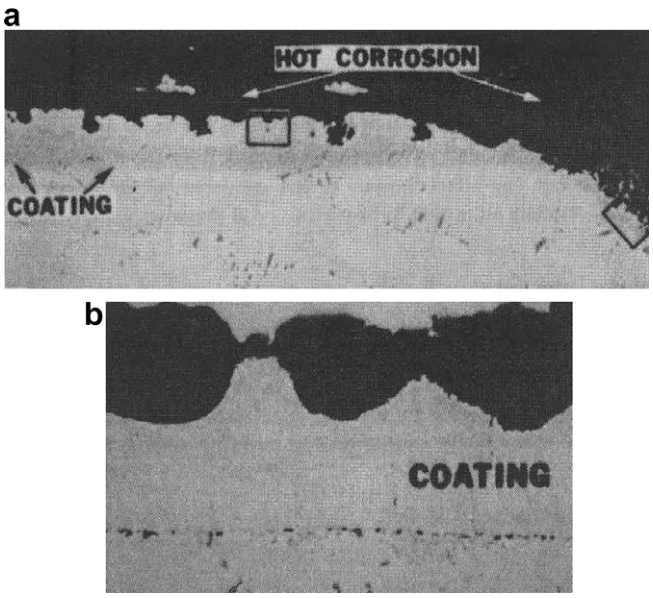

Fig. 3. Examples of hot corrosion (a) high temperature hot corrosion (aircraft engines) and (b) low temperature hot corrosion (marine and land engines).

thereby influencing hot corrosion. The cool air film adds resistance to both heat transport and mass transport from hot gas laden with sulfur compounds to the turbine component walls. At first glance this may imply that the corrosion rate would go down in the presence of film cooling, but in an earlier work reported by the authors [4] it was pointed out that the corrosion rate can even go up. The before mentioned analysis was carried out on the basis of a simple resistance model. In the present paper, the same resistance model is used to qualitatively predict the variation of LTHC rate along a film-cooled surface with a presumed distribution of effectiveness, as typically observed in heavy frame, high temperature gas turbines employed in power generation. The present work is to bring forward the regions, if any, on a hot-gas-path surface of such a turbine that may be particularly vulnerable to LTHC, in spite, of or because of film cooling.

2. Background

Hot corrosion, also called sulfidation or deposit modified corrosion, may be defined in broad terms as an accelerated, often catastrophic surface attack of hot gas path component surfaces in gas turbines, in the presence of trace amounts of sulfur derived species in the hot gas stream. Hot corrosion is typically observed in boilers, diesel engines, mufflers of internal combustion engines and gas turbines. In these cases a liquid deposit is formed on the hot surface through the condensation of salt vapors present in the hot gas stream. Depending upon the combustion process, type and purity of the fuel as well as the quality of air available the intensity of hot corrosion can vary substantially. Initially the effect of hot corrosion observed on the component surface is minimal because of the less deposition, however, the deposit once formed modifies the degradation mechanism and the reaction rate increases by an order of magnitude or more.

There is a general agreement among researchers that the presence of condensed alkali metal salts, notably Na_2SO_4 is a prerequisite to start hot corrosion. For years, corrosion problems associated with molten Na_2SO_4 have been studied in isolation with the gas turbines. The chemistry involved during the formation of Na_2SO_4 becomes highly complex in a coal or syngas fired gas turbine as discussed by Ahluwalia and co-researchers [5,6]. Sodium, as an impurity in coal, exists primarily as a halide, alumino-silicate or in combination with the organic matter. During the combustion of coal, sulfur compounds are released to render Na_2SO_4 as the only sodium containing stable condensate. There are many factors that influence the formation of Na_2SO_4 in a coal or syngas fired gas turbine system. Here we are concentrating only on two primary factors: operating temperature and mass fraction of sulfur present in the fuel.

Both the gas and hot metal surface temperatures play a major role in the formation and deposition of Na_2SO_4. The dew point temperature (T_d) of Na_2SO_4, which is inversely proportional to the sodium concentration [6], marks the onset of Na_2SO_4 deposition. Fig. 4 schematically shows the relevant transport processes that affect Na_2SO_4 deposition for different values of T_d. For a superheated gas, $T_\infty \gg T_d$, sodium containing species (NaOH and NaCl) and SO_2 diffuse towards the sub-cooled wall ($T_w < T_d$) thereby aiding sulfidation of the salts, while Na_2SO_4 diffuses outwards due to the large difference between T_∞ and T_w (with corresponding difference in partial pressures [6]). As the gas temperature reduces and approaches the dew point ($T_\infty \geqslant T_d$), a situation arises where the Na_2SO_4 starts to diffuse towards the wall, thereby reinforcing the sulfidation of NaOH and NaCl. Further decrease in the

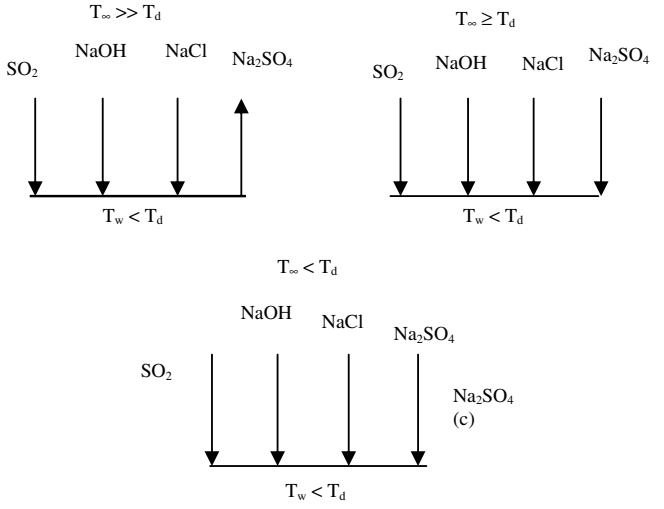

Fig. 4. Effect of temperature and sulfur mass fraction on formation of Na_2SO_4; Na_2SO_4 (c) refers to partial condensation [6].

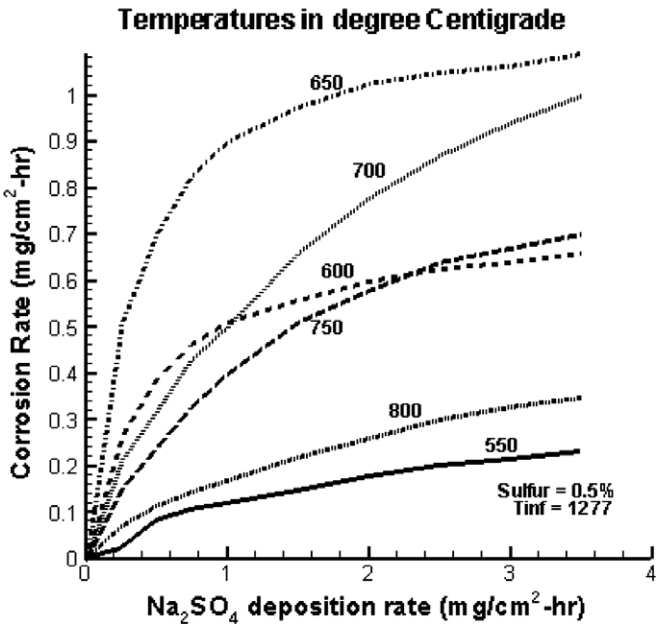

Fig. 5. Variation of corrosion rate with Na_2SO_4 deposition rate at various wall temperatures [6].

gas temperature relative to T_d will lead to the condensation of a portion of Na_2SO_4 in the vapor phase itself. The first two cases discussed above are of primary concern in high temperature gas turbine systems.

Ahluwalia and Im [6] developed a Na_2SO_4 mass transfer model and were able to predict the dependence of hot corrosion on the operating temperatures, sulfur content in the fuel and other parameters, as shown in Fig. 5. However, that work did not consider the impact of film cooling on the convective transport of the species. In fact, corrosion and heat transfer studies quite often ignored the issue of LTHC in high temperature gas turbines, based on the assumption that wall temperatures in such a turbine would be above the temperature range where LTHC is most common or damaging. This paper explores the validity of this assumption. Present study uses the results reported by Ahluwalia and Im [6] along with a simple resistance model for heat and mass transfer to establish the variation of hot corrosion rate along a surface, in the presence of film cooling for various film effectiveness distributions corresponding to different blowing ratios. The paper then identifies whether LTHC gets suppressed or augmented in the presence of film cooling. This work is a stepping stone to establish the need to study LTHC in the context of high temperature turbines using coal gas or syngas fuels containing trace amount of sulfur.

3. Analysis

In the present analysis flow over a flat plate is considered with the introduction of film cooling air through a hole, as depicted in Fig. 6. It is assumed that the boundary layer at the point of coolant introduction is turbulent and the fluids

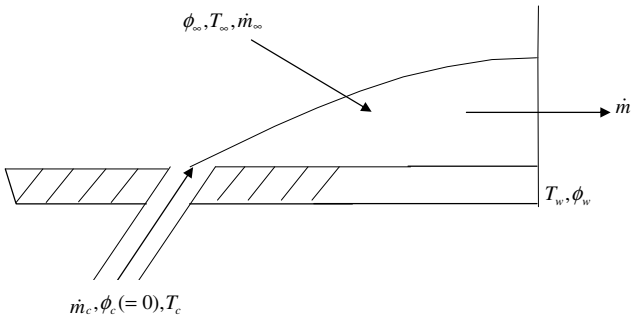

Fig. 6. Turbulent boundary layer flow over a flat plate with film cooling.

involved are gases with constant properties. The film cooling effectiveness is typically defined as

$$\eta \equiv (T_r - T_{aw})/(T_r - T_c) \quad (1)$$

where T_{aw} is the wall temperature that would be obtained beneath the film if the wall were adiabatic and T_r is the recovery temperature given as

$$T_r = T_\infty + \frac{Pr^{1/3}U_\infty^2}{2C_p} \quad (2)$$

Experimentally, there have been a lot of investigations on quantifying the film cooling effectiveness for various hole shape designs. It has been observed by researchers [3,7–9], that the film cooling effectiveness varies asymptotically along the flow direction and is dependent on the blowing ratio. With high blowing ratios the jet lifts off from the metal surface resulting in poor effectiveness close to the exit of the holes. In accordance to these observations, in the present study three representative blowing ratios: low, medium and high are considered with their corresponding effectiveness distribution depicted in Fig. 7.

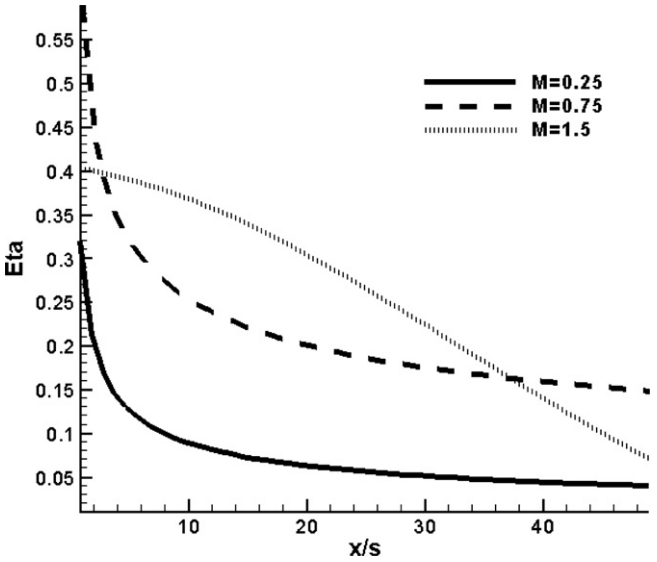

Fig. 7. Effectiveness distribution at various blowing ratios along the film-cooled surface [7].

Presence of coolant film also affects the local heat transfer coefficient. Many investigations (e.g. [7,10,11]) without looking in to corrosion effects have been reported giving variation of heat transfer coefficients in the presence of film cooling under various flow conditions. As reported by one of the investigators [7] normalized heat transfer coefficient (h_1/h_0) for three blowing ratios ($M =$ 0.25, 0.75 and 1.5) considered in the present work is depicted in Fig. 8, where h_0 and h_1 are heat transfer coefficient in the absence and presence of film cooling, respectively. In general, the heat transfer to a wall from the hot gas stream in the presence of film cooling or otherwise is characterized by the heat flux to the wall and is given by

$$q'' = h[T_{\mathrm{ref}} - T_{\mathrm{w}}] \tag{3}$$

where T_{ref} and h are the appropriate reference temperature and heat transfer coefficient, respectively. In the absence of film cooling T_{ref} is taken to be T_{r}, while in the presence of the film cooling T_{aw} is used for T_{ref}.

Following the analogy between heat and mass transfer, when considering the mass transfer process in the presence of film cooling one can define an impermeable wall mass fraction (ϕ_{iw}) as the mass fraction of the mass transfer species that would be obtained at the wall in the presence of film if the wall were impermeable to the species (i.e. there is no reaction, absorption or condensation, etc.). Based on an impermeable wall mass fraction a film protection effectiveness can be defined as

$$\eta_{\mathrm{c}} = (\phi_{\mathrm{iw}} - \phi_{\infty})/(\phi_{\mathrm{c}} - \phi_{\infty}) \tag{4}$$

A value of $\eta_{\mathrm{c}} = 1$ indicates that it is evaluated at the point of injection of the coolant, while $\eta_{\mathrm{c}} = 0$ is pertaining to a far away location.

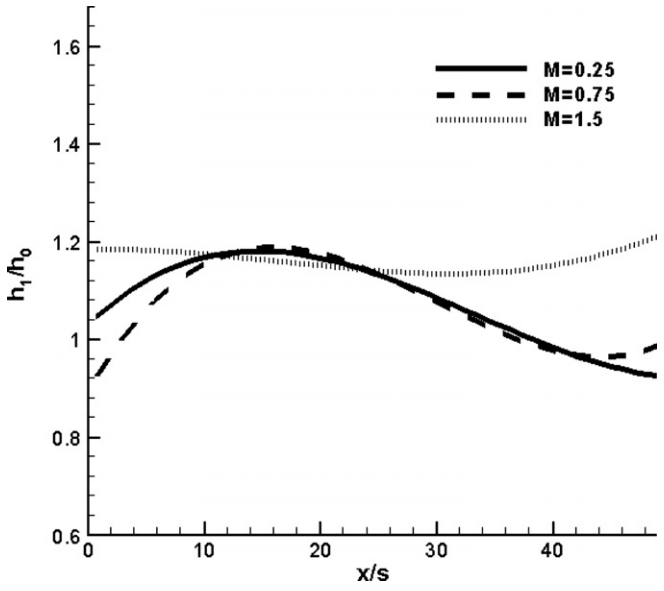

Fig. 8. Heat transfer coefficient distribution along the surface in the presence of film cooling; h_0 represents the value in the absence of film cooling [7].

Similar to the heat flux, the mass flux to the wall of a particular species can be obtained from

$$j_{\mathrm{w}} = \rho h_{\mathrm{m}}(\phi_{\mathrm{ref}} - \phi_{\mathrm{w}}) \tag{5}$$

Here ρ is the overall density and ϕ_{ref} and h_{m} are the appropriate reference mass fraction and mass transfer coefficient.

It should be noted that if Prandtl (Pr) and Schmidt (Sc) numbers are the same, and if we could ignore the difference between C_{p_∞} and C_{p_c}, then η and η_{c} will have identical values, and similarly Nusselt (Nu) and Sherwood (Sh) numbers will be equal indicating perfect analogy between heat and mass transfer [12]. In this case, the mass transfer coefficient distribution can be related to the heat transfer coefficient by

$$h_{\mathrm{m}} = \frac{h}{\rho C_p} \tag{6}$$

In the present analysis, we use this analogy and consider two cases, namely the "dry" case as a baseline wherein there is no film cooling and the "wet" case where film cooling is present. Both these cases are analyzed using the resistance model as shown in Fig. 9. Based on these resistances the wall temperature distribution and the Na_2SO_4 deposition rate distribution for the baseline and "wet" cases are estimated and corrosion rates are predicted using the results of Ahluwalia and Im [6].

The present analysis is carried out with the following conditions:

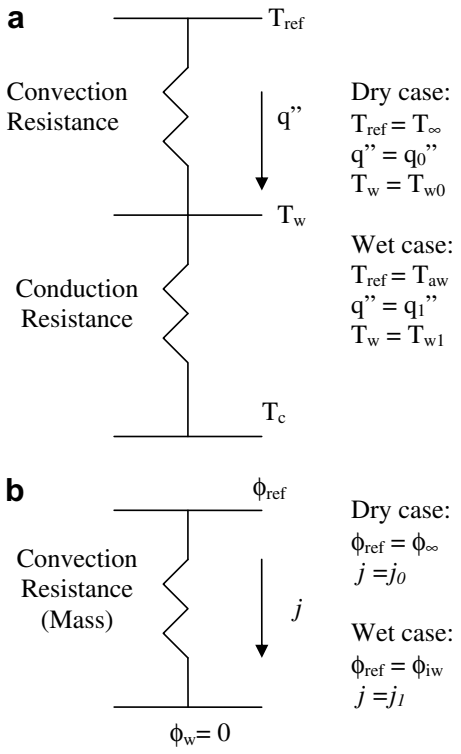

Fig. 9. Resistance model for (a) heat transfer and (b) mass transfer.

(1) The chemical process is assumed to be transport-limited rather than kinetics-limited (i.e. Damkohler number $\gg 1$). This means that as soon as the sulfur bearing precursor arrives at the wall after diffusion through the boundary layer, it is reacted upon instantaneously with no accumulation of sulfur derived precursor at the wall, leading to the formation and deposition of Na_2SO_4 and $\phi_w = 0$.
(2) It is assumed that the reaction model used by Ahluwalia and Im [6] is still valid, although the near wall and free stream temperatures are different from their analysis. As binary diffusion and thermophoresis are strong function of temperature, this assumption may not be exactly applicable. However, in the absence of generic reaction results for different values of those temperatures the present work is the first attempt for paving way towards better estimation of low temperature hot corrosion and its quantification. In view of the present status of the knowledge the objective of the paper is to establish the need of estimation of hot corrosion.
(3) Boundary layer is assumed to be turbulent enough such that effective Pr and Sc can be assumed to have same values. In other words, perfect analogy between heat and mass transport is assumed.
(4) Variation of density and specific heat is neglected. In addition it is also assumed that backside surface temperature is same as the coolant supply temperature.

Based on these assumptions using Eq. (3), where the reference temperature is the recovery temperature, and the resistance model, we can calculate the "dry" wall temperature as

$$T_{w0} = (T_c + (h_0 t_I T_r/k_I))/(1 + (h_0 t_I/k_I)) \quad (7)$$

where the heat transfer coefficient, h_0, was obtained from the literature [12]

$$Nu_x = h_0 x/k_f = 0.0296(Re_x)^{4/5}(Pr)^{1/3} \quad (8)$$

Here we have used the correlation for uniform wall temperature conditions in order to get an estimate of the convective heat (later mass) transfer coefficients without film cooling. It should be noted that in the real situation, the wall is neither at a uniform temperature, nor with uniform wall heat flux. In addition, the wall temperature distribution is not known a priory.

For the "wet" case, using the effectiveness distributions (as presented in Fig. 7) one can evaluate the variation of the adiabatic wall temperature for different blowing ratios at a given mainstream temperature, velocity and coolant temperature using Eq. (1). The adiabatic wall temperature can then be written as

$$T_{aw} = T_r + \eta[T_c - T_r] \quad (9)$$

This adiabatic wall temperature is the reference temperature in Eq. (3) for driving the heat flux to the wall in the presence of film cooling.

Plugging adiabatic wall temperature in Eq. (3) and the resistance model we can calculate the "wet" wall temperature T_{w1} as

$$T_{w1} = (T_c + (h_1 t_I T_{aw}/k_I))/(1 + (h_1 t_I/k_I)) \quad (10)$$

In the above equation, the heat transfer coefficient, h_1, is obtained from Fig. 8 and Eq. (8). In order to find the Na_2SO_4 deposition rate for both the "dry" and "wet" cases we are interested in the mass transfer of sulfur-carrying species such as SO_2 from the main flow to the wall. For this purpose we use a transport-limited reaction process where the reaction rate at the wall is fast enough (compared to the time scale of transport) so that sulfur species gets consumed instantaneously as it arrives at the wall. This gives $\phi_w = 0$. In reality, no reaction is infinitely fast and hence $\phi_w = fn\{\text{reaction rate}, T_w\}$. However, this simplification is not expected to change the qualitative conclusion obtained in the present analysis. Based on this, one can obtain the "dry" Na_2SO_4 deposition rate using Eq. (5), given as

$$j_0 = \rho h_{m0} \phi_\infty \quad (11)$$

where the reference mass fraction is ϕ_∞ and h_{m0} is obtained from Eqs. (6) and (8).

For the "wet" case, using the distribution of η_c (Fig. 7) the impermeable wall mass fraction of the sulfur-carrying species can be evaluated as

$$\phi_{iw} = \phi_\infty + \eta_c[\phi_c - \phi_\infty] \quad (12)$$

One can then compute the "wet" Na_2SO_4 deposition rate as

$$j_1 = \rho h_{m1} \phi_{iw} \quad (13)$$

Here h_{m1} is obtained from Eqs. (6) and (8) and Fig. 8.

It should be noted that the mass transfer process of SO_2 to the wall, which is related to the chemical reactions that lead to the formation of Na_2SO_4 and then hot corrosion, is not analogous to the heat transfer process into the wall. This is so because the reactions are highly non-linear functions of temperature at the wall and also binary and thermophoretic transport are dependent on temperature. However, detailed reaction models are missing from the current literature and in the absence of such models a first order approximation would be a resistance model as shown in Fig. 9b, wherein the mass flux is independent of temperature and is linearly proportional to the driving difference in mass fraction. From this "dry" wall temperature and Na_2SO_4 deposition rate distribution the variation of corrosion rate along non-cooled surface can be found using the reported results [6] and as depicted in Fig. 5. Further, using the calculated "wet" wall temperature and Na_2SO_4 deposition rate the corrosion rate for a surface in the presence of film cooling can be predicted in a similar fashion and hence the influence of film cooling on hot corrosion can be ascertained.

In the present analysis, the following parameters relevant to gas turbine engines are chosen:

(i) Mainstream temperature (T_∞) = 1425 °C (1698 K),
(ii) Sulfur mass fraction in the fuel (ϕ_∞) = 0.5%,
(iii) Mainstream velocities (U_∞) = 600 m/s and 300 m/s,
(iv) Inconel plate thickness = 0.0127 m,
(v) Inconel thermal conductivity (k) = 9 W/m-K,
(vi) Blowing ratios (M) = 0.25 (low), 0.75 (medium) and 1.5 (high).

In the present analysis, the higher velocity chosen is the same as used by Ahluwalia and Im [6], typically found in the throat region of vanes in a real engine, while for a better understanding the analysis was extended further to a lower velocity which may corresponds to an upstream region. Results were obtained for five different coolant temperatures starting from 450 °C (723 K) with an increment of 25 °C to 550 °C (823 K).

4. Results and discussion

As a baseline case, first the mainstream velocity was taken as 600 m/s, which is the same as used for corrosion analysis [6]. As stated earlier, the mass transfer process was assumed to be independent of the temperature; hence the distribution of the Na_2SO_4 deposition rate is independent of coolant temperature. However, the resistance to SO_2 transport caused by the presence of coolant film, if any, should affect Na_2SO_4 deposition rate on the metal surface. The estimated Na_2SO_4 deposition rate distribution is obtained by Eq. (11) for the "dry" case and by Eq. (13) for the "wet" cases, as given in Fig. 10. In the absence of film cooling, as the thickness of boundary layer increases, rate of SO_2 transport to the wall decreases, which should decrease Na_2SO_4 deposition rate on the surface. In the presence of film cooling the Na_2SO_4 deposition rate is influenced not only by the mass-transfer coefficient but also by the film protection effectiveness. It is easier to visualize this interaction by modifying Eq. (13) as

$$j_1 = \frac{h_1}{h_0} j_0 (1 - \eta_c) \tag{14}$$

For low blowing ratio ($M = 0.25$), where the film coverage is poor, the effect of coolant flow is predominant only in the proximity of the hole ($x/s < 2$), beyond which the effect of increasing boundary layer thickness influences the Na_2SO_4 deposition rate. It is observed that Na_2SO_4 deposition rate monotonically decreases for $x/s > 2$. However, film effectiveness is enhanced at the medium blowing ratio ($M = 0.75$) value and just downstream of the cooling hole ($x = 0^+$), the flow surface is completely covered by the coolant. As a result the SO_2 transported to the film is convected downstream. Hence, Na_2SO_4 deposition rate is almost zero at $x = 0^+$. Immediately downstream of the hole the sulfur species concentration in film increases resulting in a rapid increase in Na_2SO_4 deposition rate from $x/s = 0$. However, further downstream ($x/s > 16$) as the boundary layer becomes thicker SO_2 transport from the free stream tend to decrease. Hence, Na_2SO_4 deposition rate starts decreasing after reaching a maximum. This peak plays an important role in the subsequent corrosion process and the final conclusion of this paper. When $M = 1.5$, the cooling film is well transported due to the high momentum of the coolant flow due to which the decay in effectiveness is not very strong compared to the other blowing rates. Therefore, in the vicinity of the hole (for $x/s < 22$), the Na_2SO_4 deposition rate mainly depends on the boundary layer growth and is a weak function of the effectiveness and leads toward decrease in the Na_2SO_4 deposition rate in this range. Further downstream as the coolant flow loses momentum the effectiveness drops, however the mass transfer coefficient is further enhanced leading to the increase in Na_2SO_4 deposition rate.

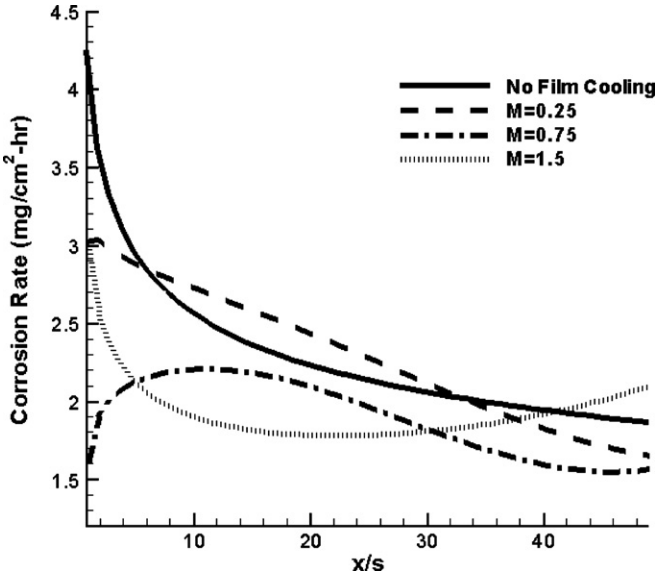

Fig. 10. Na_2SO_4 deposition rate with and without film cooling.

Fig. 11 shows the temperature distribution of the wall for the five coolant temperature cases along with the no film cooling case. Using the wall temperature distributions reported in Fig. 11 and the Na_2SO_4 deposition rate (Fig. 10) the "dry" and "wet" corrosion rates were calculated and the results are as presented in Fig. 12. Consistent with the reported results [6], the maximum surface temperature at which LTHC prevails was taken as 800 °C and above this temperature the LTHC rate was taken as zero. In the "dry" case it can be seen (Fig. 11a) that at any particular coolant temperature the surface temperature distribution decreases monotonically. When the temperatures all along the surface are in the neighborhood of 650 °C it is expected that the corrosion rate should increase, attain a maximum, and then decrease. This is because of the fact that in the range of LTHC, for a given Na_2SO_4 deposition rate, the corrosion rate increases till a particular surface temperature (in the vicinity of 650 °C [4]) beyond which it starts decreasing. However, if the surface temperature is above 650 °C the corrosion rate monotonically increases. In the "dry" case the surface temperatures are well above

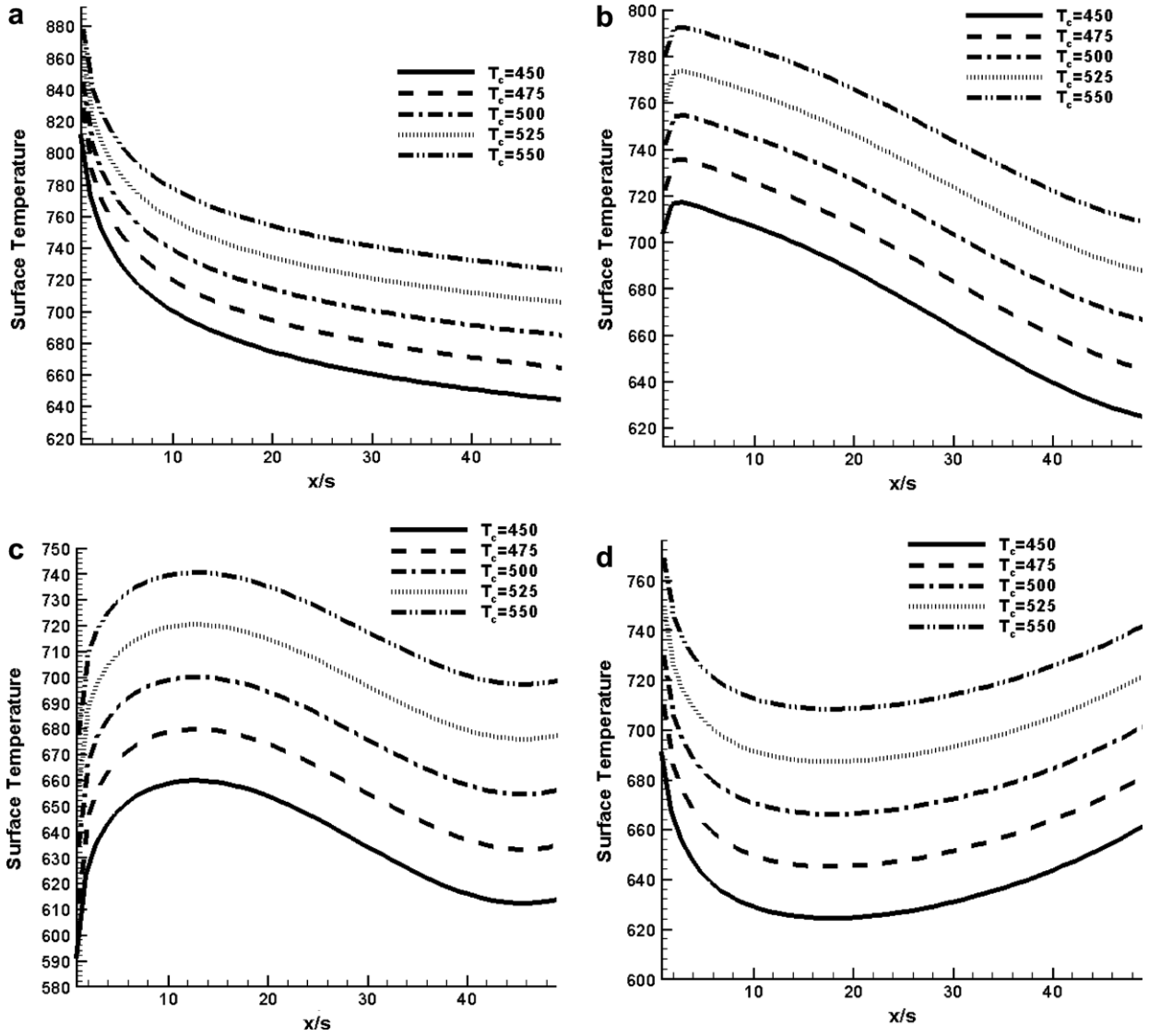

Fig. 11. Surface temperature distribution (a) without film cooling, (b) with film cooling, at $M = 0.25$, (c) at $M = 0.75$ and (d) at $M = 1.5$ (temperatures in °C).

650 °C and hence the hot corrosion rate monotonically decreases as depicted in Fig. 12a.

In "wet" cases, depending on the blowing ratio, the temperature distribution takes the form as shown in Fig. 11b–d. The corresponding calculated corrosion rates are shown in Fig. 12b–d. At low blowing ratio, $M = 0.25$, both the surface temperature and Na_2SO_4 deposition rate increase very close to the hole. At these locations the corrosion rate decreases. This is due to the fact that the surface temperatures are greater than 650 °C leading to the reduction in the corrosion rate. Beyond $x/s = 2$ the corrosion rate starts to increase monotonically. This trend is observed for all the coolant temperatures greater than or equal to 475 °C. However, when the coolant temperature is 450°C the corrosion rate increases till it attains a maximum (in the vicinity of 650 °C) beyond which it starts decreasing again. This is due to the fact that the surface temperatures are on either side of 650 °C. It should be noted here that the sudden jumps in corrosion rate at certain places is due to discontinuities in the obtained data.

For $M = 0.75$, at all the coolant temperatures, corrosion rate peaks very close to the hole and is highest for the lowest temperature, $T_c = 450$ °C. At this blowing ratio the wall temperatures are in the neighborhood of 650 °C and hence the distinctive peaks in the corrosion rate. Moreover, the Na_2SO_4 deposition rate also increases close to the hole, which significantly contributes to the augmentation of the corrosion rate. Once the surface temperature and Na_2SO_4 deposition rate start decreasing the corrosion rate also decreases.

At $M = 1.5$, when $T_c \geqslant 500$ °C, the corrosion rate shoots up very close to the hole. As we go downstream the corrosion rate continues to increase until about $x/s = 14$ beyond which it starts to decrease. For coolant temperatures below 500 °C the corrosion rate peaks initially, and then decreases till x/s close to 20 beyond which it

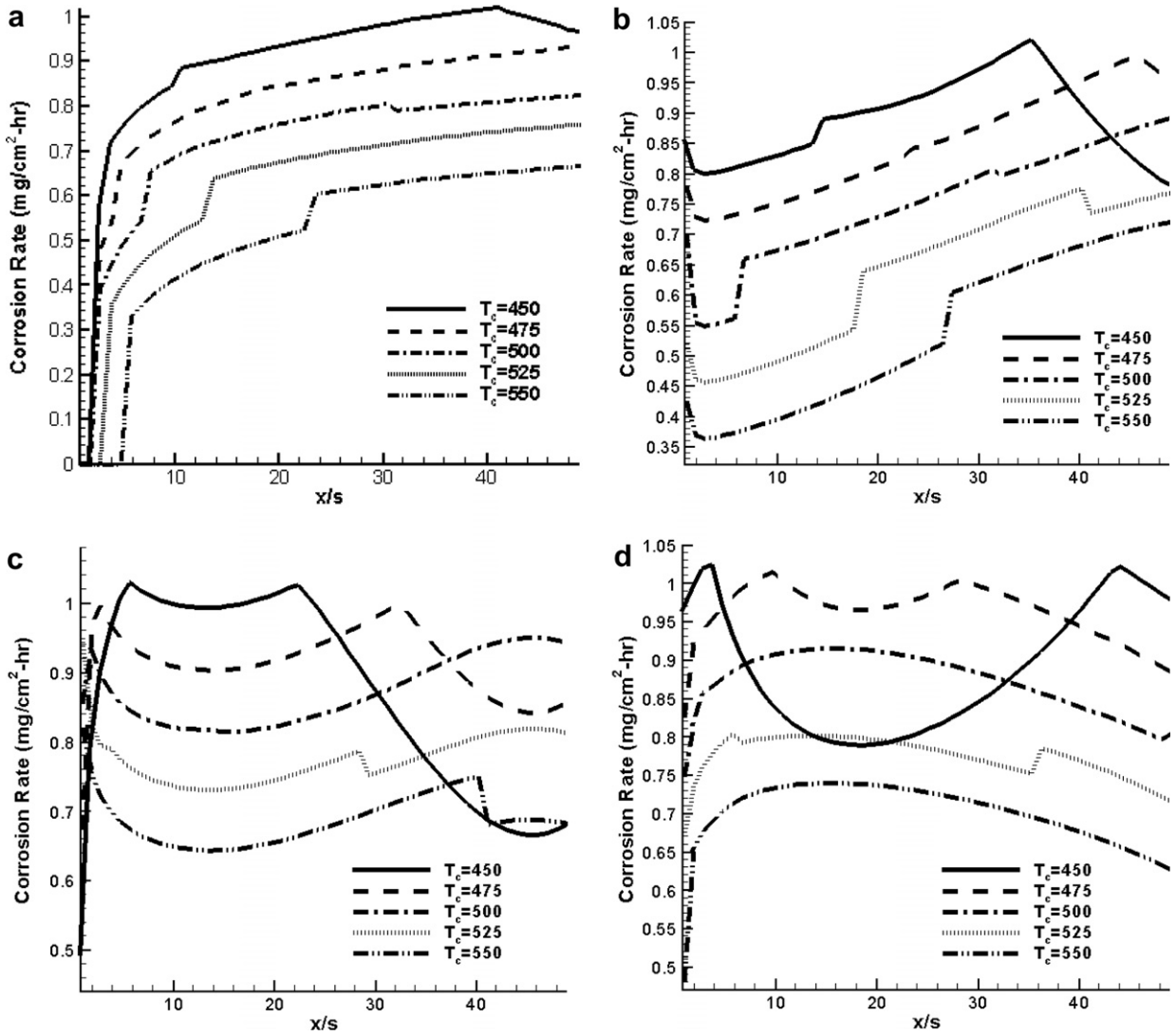

Fig. 12. Corrosion rate (a) without film cooling, (b) with film cooling, at $M = 0.25$, (c) at $M = 0.75$ and (d) at $M = 1.5$ (temperatures in °C).

increases once again. As we go further downstream the corrosion rate begins to fall once again. This peculiar trend at these low coolant temperatures is due to the fact that the surface temperatures vacillate in the proximity of 650 °C.

A better comparison is revealed by the cross-plot of the corrosion rates, without and with film cooling for four film coolant temperatures, as shown in Fig. 13a–d. From Fig. 13a, which depicts the corrosion rate with and without film cooling at a coolant temperature of 450 °C, we can see that the LTHC rate increases dramatically after the application of film cooling especially close to the hole opening. In fact for $M = 0.75$ LTHC rate is higher than the no film cooling case until x/s of 25. The reason for the increase in the corrosion rate for $M = 0.75$ is that, once film cooling is employed, the surface temperature and the Na_2SO_4 deposition rate are lowered. In particular close to the hole the temperatures before film cooling are outside the domain of LTHC. However, with film cooling the temperatures drop to values which are much closer to 650 °C and so the corrosion rate increases at these locations [4]. However, when $M = 0.25$ the film coverage is poor and hence the reduction in surface temperature is not significant to alter the corrosion process. Therefore, no profound effect in corrosion rate is observed. When $M = 1.5$, although the corrosion rate peaks in the vicinity of the injection hole, beyond $x/s = 10$ it is lower than its corresponding "dry" case due to the low temperature and Na_2SO_4 deposition rate.

When the coolant temperature is at or higher than 475 °C, irrespective of the blowing ratio the corrosion rate is higher than the no film cooling case in the vicinity of the point of coolant injection, where the effectiveness is maximum as observed in Fig. 13b–d. However, as we go downstream the corrosion rate continues to be higher than the no coolant counterpart for $M = 0.75$ and 1.5, while for $M = 0.25$, beyond x/s of 7, there is no appreciable effect of film cooling on the corrosion rate due to poor coverage.

Analysis was carried out for yet another mainstream velocity, namely 300 m/s as stated earlier. This value was chosen in order to use the same effectiveness plot. The analysis was performed to ascertain the effect of the mainstream

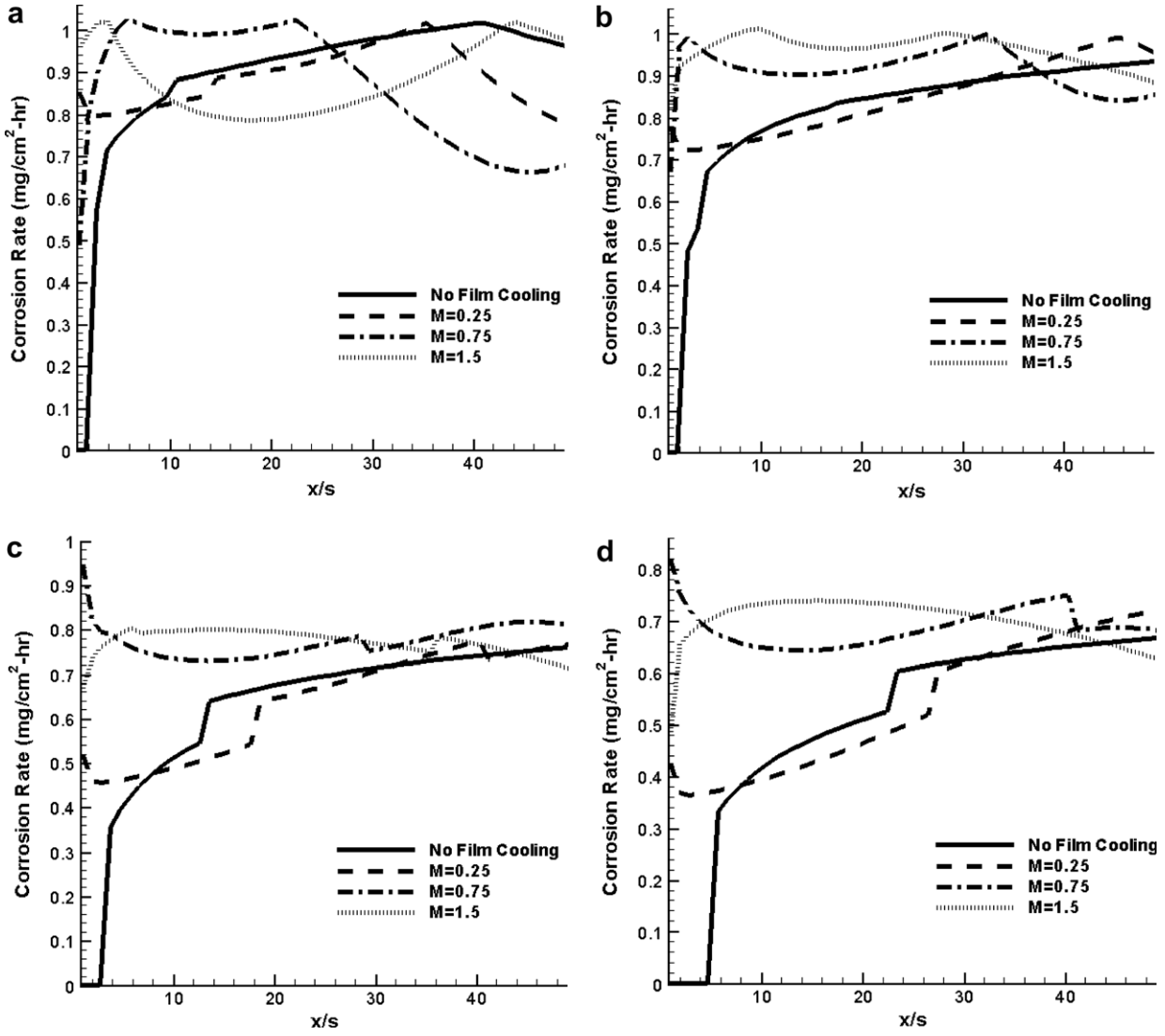

Fig. 13. Hot corrosion rate with and without film cooling at various coolant temperatures (a) $T_c = 450$, (b) $T_c = 475$, (c) $T_c = 525$ and (d) $T_c = 550$ (temperatures in °C).

velocity on the Na_2SO_4 deposition rate and surface temperature and hence eventually the corrosion rate. The mainstream velocity alters the transport of heat as well and species into the boundary layer. As a result the deposition rate of sodium sulfate and the surface temperature changes. The Na_2SO_4 deposition rate at 300 m/s is depicted in Fig. 14 along with the Na_2SO_4 deposition rate for the "dry" case. It can be seen from this plot that the injection of coolant flow reduces the transport of sulfur derived species and hence reduces the Na_2SO_4 deposition rate and the trend is similar to that of mainstream velocity 600 m/s. However, the amount of deposition is significantly less. Similarly the surface temperatures at a velocity of 300 m/s follow the same trend as that when the velocity is 600 m/s, but the magnitudes are lower. The surface temperature distribution is shown in Fig. 15 for both "dry" and "wet" cases for the lower velocity case.

Based on the Na_2SO_4 deposition rate and the surface temperature distribution the corrosion rate for this velocity

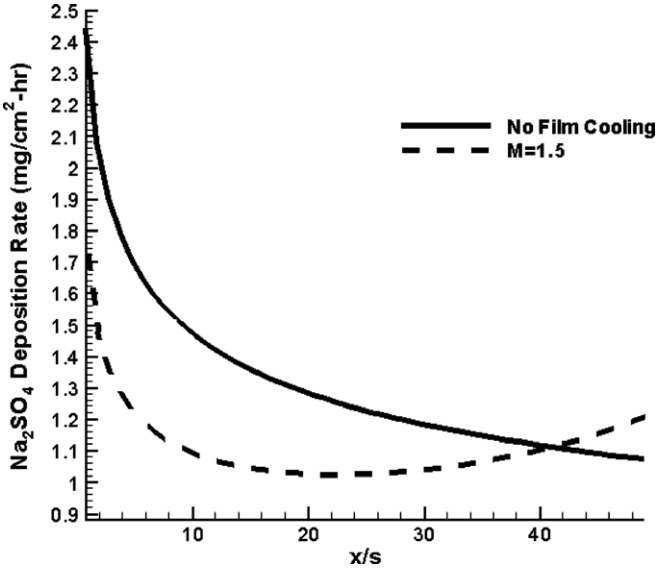

Fig. 14. Na_2SO_4 deposition rate for mainstream velocity of 300 m/s.

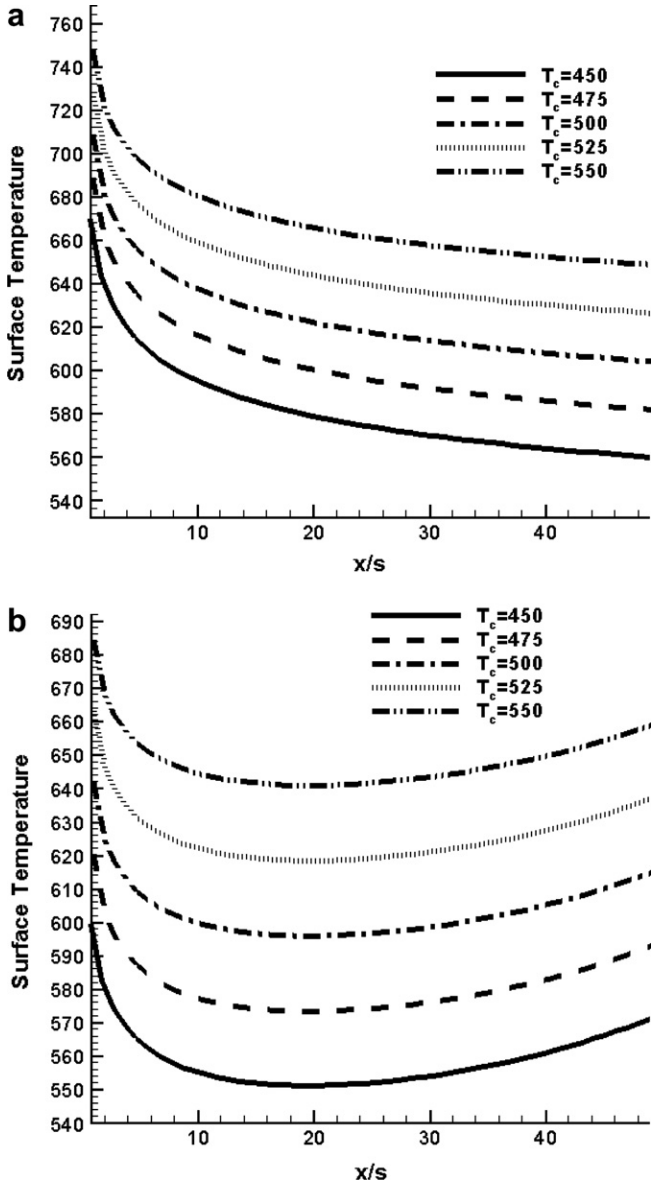

Fig. 15. Surface temperature distribution for mainstream velocity of 300 m/s: (a) no film cooling and (b) $M = 1.5$. (temperatures in °C).

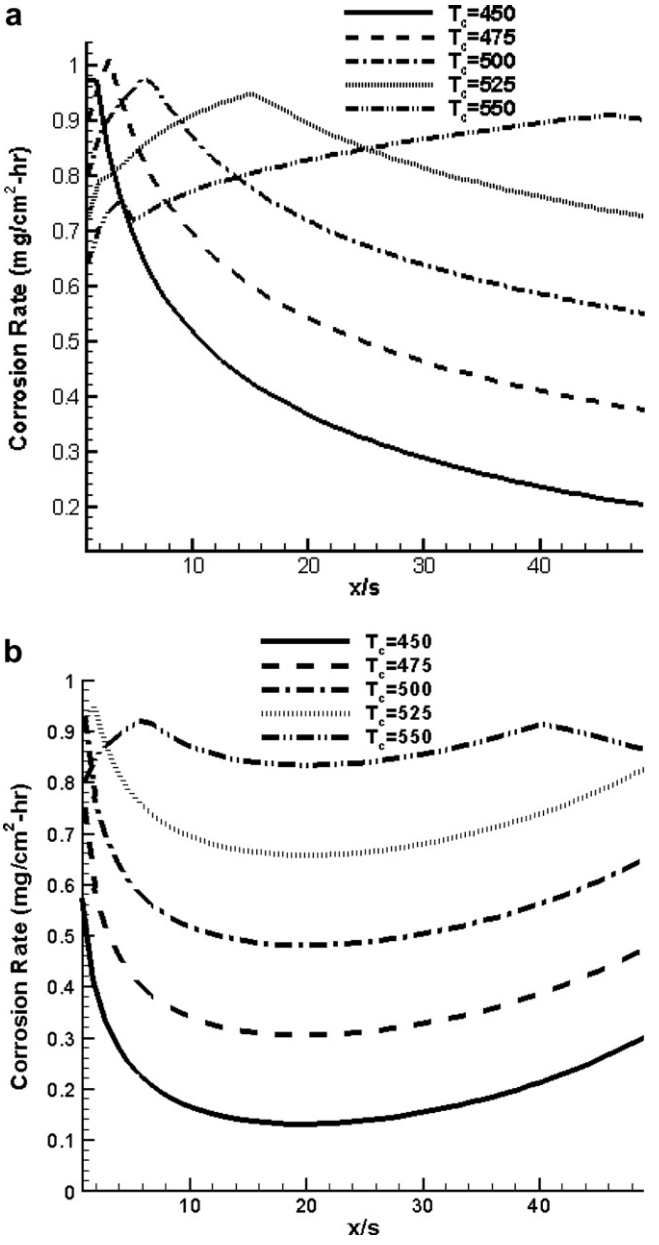

Fig. 16. Corrosion rate for mainstream velocity of 300 m/s: (a) no film cooling and (b) $M = 1.5$ (temperatures in °C).

was obtained following the procedure described for the higher velocity. The corrosion rates for a blowing ratio of $M = 1.5$, for the different coolant temperatures is shown in Fig. 16. The corrosion rate for all the cooling temperatures, except $T_c = 550$ °C, reduces in the vicinity of the cooling hole and increases around $x/s > 20$. When $T_c = 550$ °C, the corrosion rate peaks at the vicinity of the cooling hole and then stays fairly constant.

Although the surface temperature and the Na_2SO_4 deposition rate followed similar trends in both the velocity cases, it can be seen from the respective corrosion rate plots (Figs. 12 and 16) that the corrosion rates behave very differently. In the former case (600 m/s, $M = 1.5$), the corrosion rate peaked very close to the hole for all the coolant temperatures. In fact, near the hole, it was highest for $T_c = 450$ °C. In comparison, the corrosion rates for the latter case (300 m/s, $M = 1.5$), are lower for lower coolant temperatures. Hence, it can be seen that, film cooling can either increase or decrease the hot corrosion rate. Moreover, the choice of operating parameters could significantly affect the LTHC rate. Therefore the need arises to properly choose the operating parameters to prevent LTHC and increase the operating life of gas turbines. However, optimizing the design is beyond the scope of the present work.

5. Conclusions

The variation of LTHC rate along a hot-gas-path surface in a gas turbine and the influence of film cooling on this corrosion rate were studied. To accomplish this

objective, a simple resistance model with a general film cooling effectiveness distribution and heat transfer coefficient enhancement distribution for various blowing ratios was employed. In the absence of a rigorous model available in the present literature, the present analysis is a step to demonstrate the possibility of understanding and predicting LTHC even with a simplistic approach. Based on the present model following conclusions are drawn:

(1) In the absence of film cooling, the corrosion rate along the surface increases for all the chosen backside temperatures as the boundary layer gets thicker and due the combined effects of surface temperature and the Na_2SO_4 deposition rate.
(2) When film cooling is employed, it impedes both the heat and mass transfer processes. However, depending upon the blowing ratio, mainstream velocity and coolant temperature, the corrosion rate could either increase or decrease. Although $M = 0.75$ seems to be an optimum blowing ratio (as it provides good film coverage), it could prove detrimental with regards to LTHC.
(3) With film cooling, there is a sharp rise in the corrosion rate close to the cooling hole (within $10s$). Due to the possibility that the base super alloy may be exposed in this region, designers should consider the high corrosion rate seriously.
(4) While the corrosion rate peaks close to the hole for a mainstream velocity of 600 m/s, it significantly drops as the velocity is lowered (300 m/s).
(5) Although film cooling is a common technique to reduce the surface temperature, it could prove detrimental with respect to low temperature hot corrosion, which is evident from the results obtained in the present study. Therefore results obtained here call for proper optimization of the operating conditions and design methodology, particularly for turbines burning coal gas or syngas.

This study may not be quantitative in nature but still gives an insight into the need for optimizing the design in coal fired gas turbines. The present model is simple as it is based on the temperature independent reaction model, while in reality the reactions are non-linear functions of temperature, which could vary the operating parameters significantly. Moreover, the backside temperature was assumed to be equal to the coolant temperature. However, in reality, the backside temperature would be colder than T_c. This would affect the wall temperature and hence the LTHC rate. Therefore, in order to provide quantitative output for design optimization, a more sophisticated reaction model is necessary.

Acknowledgement

The first author likes to acknowledge the SWPC/UCF doctoral fellowship made available by SWPC. In addition, authors would also like to acknowledge an ongoing project on endwall film cooling jointly funded by SWPC and the Florida High Tech Corridor program, which in a way inspired the work presented here.

References

[1] F.S. Pettit, C.S. Giggins, Hot corrosion, in: C.T. Sims, N.S. Stoloff, W.C. Hagel (Eds.), Superalloys II, John Wiley & Sons, New York, 1987, Chapter 12.
[2] R.T. Jones, Thermal Barrier Coatings, in: K.H. Stern (Ed.), Metallurgical and Ceramic Protective Coatings, Chapman and Hall, London, 1996, pp. 194–235.
[3] R.J. Goldstein, Film cooling, in: T.F. Irvine, J.P. Hartnett (Eds.), Advances in Heat Transfer, vol. 7, Academic Press, New York, 1971, pp. 321–379.
[4] Vaidyanathan Krishnan, J.S. Kapat, Y.H. Sohn, V.H. Desai, Effect of film cooling on low temperature hot corrosion in a coal fired gas turbine, in: GT-2003-38693, Proceedings of ASME Turbo Expo 2003, June 16–19, Atlanta, USA, 2003.
[5] R.H. Ahluwalia, K.H. Im, C.F. Chuang, H.K. Geyer, T.J. O'Brien, G.F. Berry, Behavior of coal ash and alkali matter in a coal-fired gas turbine system, in: ASME Gas Turbine and Aeroengine Congress, The Netherlands, 1984.
[6] R.K. Ahluwalia, K.H. Im, Correlation between sodium sulfate mass transfer and low-temperature hot corrosion, in: ASME Gas Turbine and Aeroengine Congress, The Netherlands, 1988.
[7] J. Dittmar, A. Schulz, S. Wittig, Assessment of various film-cooling configurations including shaped and compound angle holes based on large-scale experiments, Journal of Turbomachinery 125 (2003) 57–64.
[8] R.S. Bunker, Effect of partial coating blockage on film cooling effectiveness, in: 2000-GT-244, ASME IGTI Conference, Munich, Germany, 2000.
[9] A.J.H. Teekaram, C.J.P. Forth, T.V. Jones, Film cooling in the presence of mainstream pressure gradients, Journal of Turbomachinery 113 (1991) 484–492.
[10] In Sung Jung, Joon Sik Lee, P.M. Ligrani, Effect of bulk flow pulsations on film cooling with compound angle holes: heat transfer coefficient ratio and heat flux ratio, Journal of Turbomachinery 124 (2002) 142–151.
[11] S. Baldauf, M. Scheurlen, A. Schulz, S. Wittig, Heat flux reduction from film cooling and correlation of heat transfer coefficients from thermographic measurements at engine like conditions, Journal of Turbomachinery 124 (2002) 699–709.
[12] E.R.G. Eckert, R.M. Drake Jr., Analysis of Heat and Mass Transfer, Hemisphere Publishing Corporation, New York, USA, 1987.